SEMARAK ILMU PUBLISHING

Journal of Advanced Research in Applied Sciences and Engineering Technology

Journal homepage:
https://semarakilmu.com.my/journals/index.php/applied_sciences_eng_tech/index
ISSN: 2462-1943


# Analysis of Control Strategy Based on P&O Algorithm for the Switching Component of Wireless Solar Power Transfer

Muhammad Irwanto[1,2,*], Nor Hanisah Baharuddin[2], Mahdi Syukri[3], Yoga Tri Nugraha[1]

[1] Department of Electrical Engineering, Faculty of Sains & Technology, Universitas Prima Indonesia (UNPRI), Medan, Indonesia
[2] Fellow of Center of Excellence for Renewable Energy (CERE), Universiti Malaysia Perlis (UniMAP), Perlis, Malaysia
[3] Department of Electrical and Computer Engineering, Universitas Syiah Kuala (USK), Banda Aceh, Indonesia

**ABSTRACT**

Previous researchers have studied wireless power transfer (WPT), while the current study focused on converting DC voltage to AC voltage on the transmitting coil and transferring it to the receiving coil. Previous studies did not discuss the control technique to drive the switching component on the converter circuit, especially the change controller in DC voltage and current affecting the WPT performance. This paper discussed a control strategy based on the P&O algorithm for driving MOSFETs on the half H-bridge inverter of a wireless solar power transfer (WSPT) system. This system is constructed by PV modules as the main DC voltage source, a control strategy based on the perturb and observe (P&O) algorithm, a half H-bridge inverter, and a transmitting and receiving circuit. The WSPT system was modelled using MATLAB SIMULINK with various solar irradiance, and its performance was assessed. The results show that the change in the total output voltage and power of PV modules can be controlled by the P&O algorithm as the signal input of the PWM generator applied to drive the MOSFETs. There are no transient values of voltage waveform on the transmitting and receiving circuit when the transient total output voltage of PV modules occurs. It indicates that the P&O algorithm can effectively manage the PWM generator for its input signal, including the total output voltage and current produced by PV modules.

***Keywords:***
Solar irradiance; wireless power transfer; wireless solar power transfer; control strategy; P&O algorithm

## 1. Introduction

Solar energy is a form of renewable energy designed to substitute traditional energy sources, which are expected to decline globally. Numerous researchers have examined solar power due to its accessibility and significant potential for serving as an alternative energy source, particularly in generating electricity. Solar energy prediction has been assessed by [1] proposing a novel model which considers sunshine duration in regions of China. The main objective of prediction is to obtain the solar energy data required to develop a photovoltaic (PV) power plant in China. The collected and analysed solar energy data show that China's western region has great potential for developing PV power plants. Modelling of solar energy prediction is also conducted by [2] using a machine learning

* *Corresponding author.*
*E-mail address: muhammadirwanto@unprimdn.ac.id*

https://doi.org/10.37934/araset.57.2.134145

algorithm. It is observed based on the three scenarios, namely uniform variation, grid variation and random variation. A genetic algorithm is also applied to optimise their required parameters. The real data on solar energy was obtained from the Concordia University, Canada campus and compared to the proposed modelling. The result showed that an accuracy of 94% was achieved for predicting solar energy, and the best model was based on random variation.

The need for solar energy data in its prediction is due to the limited availability of existing data. The prediction can be conducted by [3] using empirical formulations, [4] using ANFIS, and [5] using the model of Gumbel probabilistic. The empirical formulas by [3] contain the amount of cloud and duration of sunshine, and they are applied to four climate conditions (forest, coastal, transition, and savannah) in Ghana for the amount of cloud and duration of sunshine from 2015 to 2018. The predicted solar energy for transition and savannah is up to 22 $MJ/m^2$ or 6.1 $kWh/m^2$ compared to transition and forest climatical conditions. An ANFIS method based on the maximum and minimum temperature is applied to predict solar energy in Medan, North Sumatra, Indonesia [4]. The measured and predicted solar energy data were compared to prove that the ANFIS method can be accepted for predicting solar energy. The findings show that the ANFIS approach is acceptable, given the 2.769% error margin. Due to the measurement limitation of solar energy data by the government in Nigeria, thus a model of Gumbel probabilistic is applied [5]. The result showed that the model accurately predicted solar energy and that the data could be used to develop the Nigeria PV power plant.

The availability of solar energy data in a particular region can help assess the feasibility of establishing a PV power plant in that area. PV power plants' main electrical energy source is PV modules. They can be connected in series or parallel to obtain their required total voltage, current and power. The performance of PV modules depends on the solar energy achieving their surface. The PV modules can be applied to DC or AC loads. The DC loads can be connected directly to the PV module or using the battery to store the electrical energy from the PV modules and connected to the DC loads. An inverter circuit is needed to convert the output voltage of PV modules to the AC voltage when connected to the AC loads. Previous researchers have conducted some applications of PV modules. The PV modules were applied to the domestic hot water by [6] with a power capacity of 1 MW, and a Fuzzy controller was applied to the pumping system by [7]. A battery charging system using a PV module based on the DC-DC converter is studied by [8]. The simulation and analysis of converting DC voltage from the inverters with PV modules to an AC multilevel voltage waveform were conducted by [9, 10] using MATLAB SIMULINK. In addition, the use of PV modules for power transfer has been analysed by [11-14], focusing on applying electromagnetic principles in a wireless solar power transfer (WSPT) system.

Normally, the WSPT system is constructed by an inverter circuit, a transmitting circuit, a receiving circuit, and PV modules that can be connected in series or parallel to obtain the required power [15]. Some types and methods of WSPT systems have been studied. Self-resonant with three coils was studied by [16,15], an orientation magnetic field and position method of transmitting coil have been developed by [17], and a concept of magnetic and electric coupling between the transmitting and receiving circuit has been developed by [18-22]. Pulse generators are commonly used to study different types and approaches for simulating the WPT system, whereas microcontrollers play a key role in hardware configuration. It is important to note that there is currently no provision for introducing a feedback signal into the switching component of the inverter circuit in the WPT system (converting the DC voltage to AC voltage [23]).

This paper proposed a control strategy for the switching component of the inverter circuit on the WSPT system based on the P&O algorithm. The P&O is the abbreviation of perturb and observe, and it is an algorithm created for some conditions of some controlled variable [24,25]. The WSPT system is modelled using MATLAB SIMULINK, consisting of PV modules, an inverter circuit, and a transmitting

and receiving circuit. The P&O algorithm has two input signals from the total output voltage and current of PV modules.

## 2. Methodology

The modelling of wireless solar power transfer (WSPT) and the proposed control strategy for switching components based on the P&O algorithm are explained in this section. The WSPT was constructed using photovoltaic (PV) modules as a main DC voltage source, a half H-bridge inverter (HBI), and a transmitting and receiving circuit. The circuit of HBI has two MOSFETs as switching components. Their gate terminal needs to be driven by pulse waves and controlled by the P&O algorithm, with its two inputs from the voltage and current of the PV modules, as shown by the block diagram in Figure 1. MATLAB SIMULINK was used to simulate the performance of WSPT with the control strategy of switching components based on the P&O algorithm.

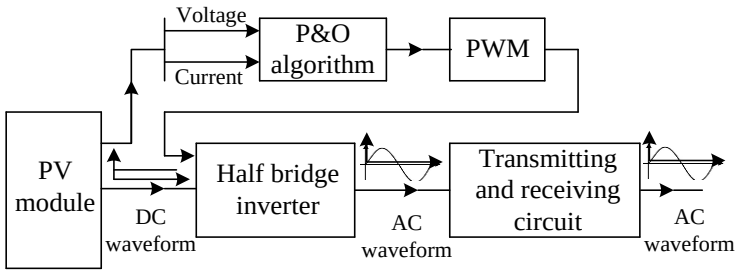


**Fig. 1.** Block diagram of control strategy based on P&O algorithm

### *2.1 Proposed Control Strategy Based on P&O Algorithm*

The P&O algorithm serves as a control method for two MOSFETs in the half-bridge circuit, requiring pulse waves to activate their gate terminal on the WSPT. The P&O algorithm is proposed to control the output voltage (*V*) and current of the PV module (*I*), whose main objective is to achieve the maximum output power of the PV module. It follows a criterion of looping process as shown by a flow chart of research methodology in Figure 2.

The output power of the PV module (*P*) is a multiplication result of the output voltage and current of the PV module. When the output power is not equal to 0, there are four change conditions of output voltage and power of PV module to decide a possibility value of duty cycle, *D* of pulse wave modulation (PWM) with its frequency is 5000 Hz following Figure 2. The first condition is if the change in *P* and *V* is lower than 0, the value of duty cycle, *D* (the old duty cycle, $D_{old}$ - the change in duty cycle, Δ*D*) will be decreased. The second condition is if the change in *P* is lower than 0 and the change in *V* is higher than 0, the value of duty cycle, *D* (the old duty cycle, $D_{old}$ + the change in duty cycle, Δ*D*) will be increased. The third condition is if the change in *P* is higher than 0 and the change in *V* is lower than 0, the value of duty cycle, *D* (the old duty cycle, $D_{old}$ + the change in duty cycle, Δ*D*) will be increased. The last condition is if the change in *P* is higher than 0 and the change in V is higher than 0, then the value of duty cycle, *D* (the old duty cycle, $D_{old}$ - the change in duty cycle, Δ*D*) will be decreased.

The PWM with a frequency of 5000 Hz and duty cycle of 50% is required to drive the gate terminal of MOSFETs in the circuit of HBI, as shown in Figure 1. The circuit converts the DC voltage of PV modules to a pure sinusoidal AC waveform on both the transmitting and receiving circuits.

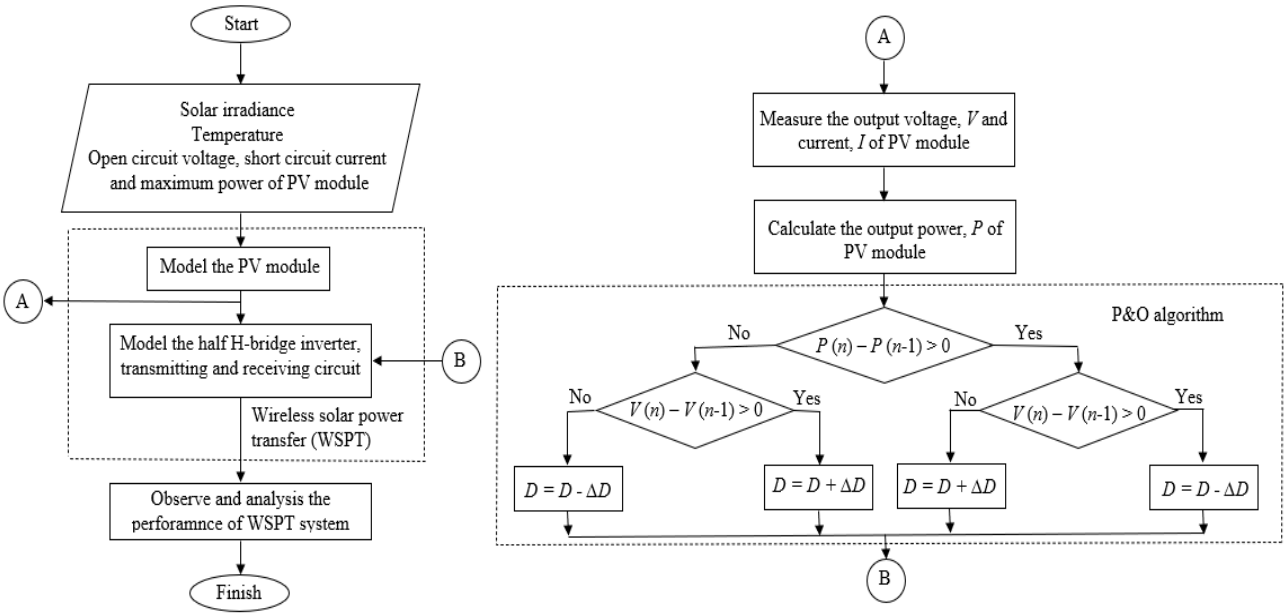


**Fig. 2.** Flow chart of research methodology

### *2.2 Modelling of Control Strategy Based on P&O Algorithm on the WSPT*

Figure 3 shows the modelling of the control strategy based on the P&O algorithm on the WSPT using MATLAB SIMULINK. The P&O algorithm was modelled using a block set of MATLAB functions to create a listing program, as stated in Figure 2. A PV module has an open circuit voltage of 21.5 V, a short circuit current of 6.52 A, and ten PV modules connected in series as modelled in the block of the control voltage source. Thus, the total output voltage of 215 V and current of 4.91 A as the input function in the P&O algorithm should be stated early in the listing program. The multiplication of total output voltage and current is equivalent to the total output power of PV modules. The possibility value of the duty cycle was determined by considering any variations in the total output power and voltage, based on Figure 2, and then used as an input signal for the PWM generator block shown in Figure 3.

The PWM generator was set to generate the pulse wave with a frequency of 5000 Hz and a duty cycle of 50%. These parameters were maintained to have fixed values for every change in the total output power and voltage. The pulse wave was applied in the HBI circuit, especially for both MOSFET gate terminals. Since the MOSFETs should be driven for the different levels of pulse waves, one of them should be inverted using NOT gate (block set of logical operator), as shown in Figure 3. It is due to an inductor of 100 µH being connected to the centre tap of the transmitting coil (its function is as a filter). Thus, the HBI circuit can convert the total output DC voltage of PV modules into a pure sinusoidal voltage waveform on the transmitting and receiving circuit.

The modelling was simulated for 0.02 s with a constant temperature of 25$^{o}$C. The initial solar irradiance is 1000 W/m$^2$, and the time of 0.01 s goes down to 100 W/m$^2$. The change in solar irradiance and temperature affects the output voltage and current of PV modules. The P&O algorithm responds to them to ensure the pulse wave is always maintained in the frequency and duty cycle of 5000 Hz and 50%, respectively. Furthermore, this condition affects the performances of PV modules and the WSPT. These performances were observed and analysed, especially at the time of change in the solar irradiance.

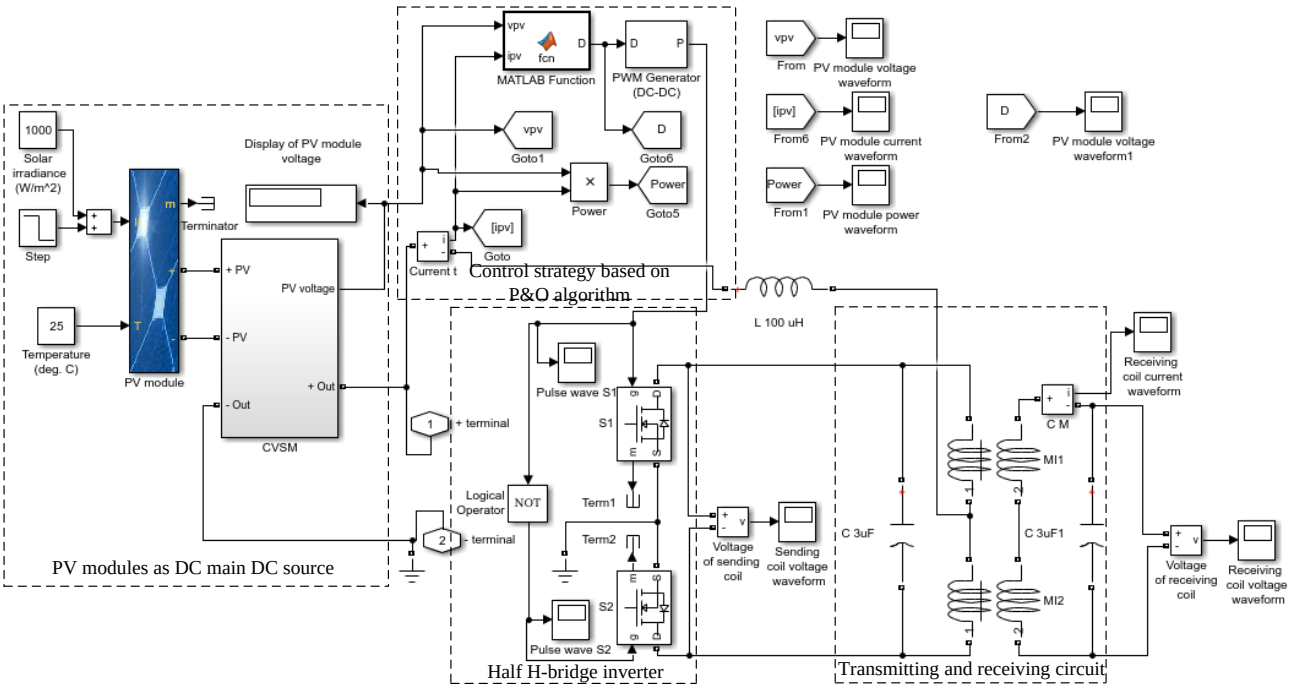


**Fig. 3.** Modelling of control strategy based on P&O algorithm on the WSPT

## 3. Results

This section shows and discusses the simulation results of the PV module and WSPT performance as an application of the control strategy of switching components based on the P&O algorithm. The discussion starts by showing the constant temperature and the solar irradiance change, which affects PV module performance. The pulse waves applied to the gate terminal of MOSFETs are also discussed in relation to the output voltage and current of PV modules. Lastly, the performance of WSPT on the transmitting and receiving circuit is also shown and discussed in this section for change of solar irradiance, which has been responded to by the P&O algorithm as the input signal of the PWM generator.

### *3.1 The Output Voltage and Current of PV Modules as the Change Effect of Solar Irradiance*

The solar irradiance of 1000 W/m$^2$ was simulated and applied to the WSPT from 0 s to 0.01 s for the temperature of 25 $^o$C, as shown in Figure 4. The solar irradiance goes down by 100 W/m$^2$ from 0.01 s to 0.02 s, but the temperature is maintained at 25$^o$C. The fluctuation of solar irradiance affects the output voltage and current of PV modules. Normally, for a constant temperature, the increasing solar irradiance causes an increase in the output voltage and current of PV modules. In contrast, reduced solar irradiance leads to decreased output voltage and current from PV modules.

The PV module output voltage of 233.6 V was generated when the solar irradiance of 1000 W/m$^2$ and the temperature of 25 $^o$C during the time 0.01s as shown in Figure 5(a) while the PV modules flow their current of 6.516 A ((7.576+5.456):2= 6.516 A) as shown in Figure 5(b). The PV module surface receives a solar irradiance of 100 W/m$^2$ at a temperature of 25 $^o$C, as shown in Figure 4. These parameters affect the output voltage and current of PV modules, where their values fluctuate from 0.01 s to 0.01002 s. Initially, the transient voltage and current occur at 0.01 s, where the negative voltage value of -2000 V (lower than 0) and the current of 1.11 A were observed. The negative voltage value occurred due to potential induced degradation (PID) in the PV modules at 0.01 s. The negative voltage value indicates that the total output power is negative or lower than 0. In this condition, the

P&O algorithm takes action to control the values following the algorithm as stated in Figure 2, where if the change in *P* is lower than 0 and also the change in *V* is lower than 0, thus decreases the value of duty cycle, *D* (the old duty cycle, $D_{old}$ - the change in duty cycle, Δ*D*). The P&O algorithm was utilised to determine the appropriate reduction of the duty cycle (*D*) and instruct the PWM generator (see Figure 3) to sustain an output frequency of 5000 Hz with a duty cycle of 50%.

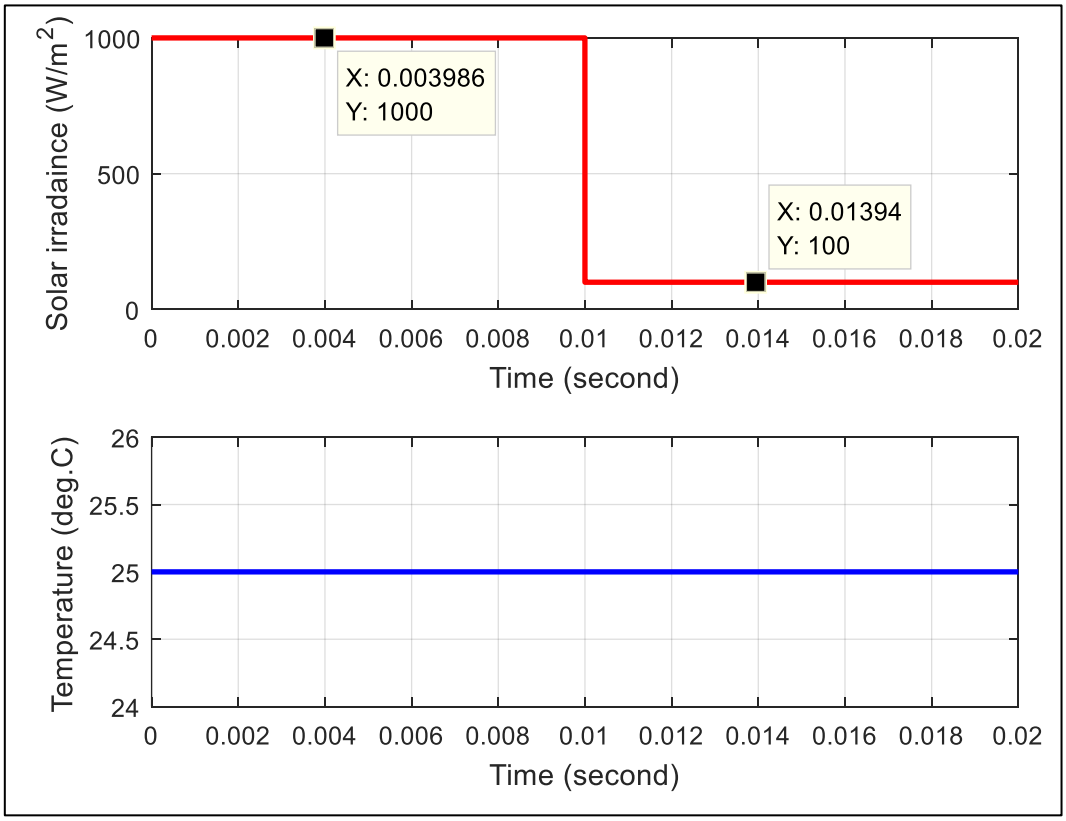


**Fig. 4.** Solar irradiance and temperature applied into the WSPT

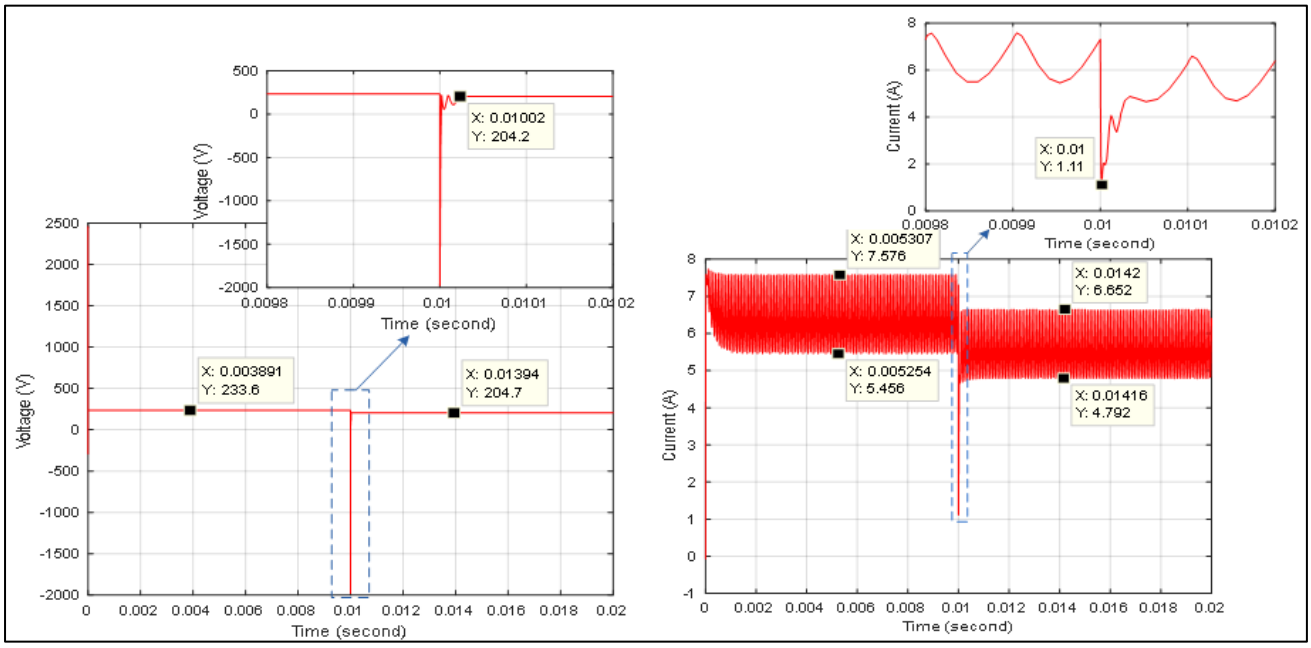


(a) (b)

**Fig. 5.** PV modules (a) Output voltage (b) Current

The output voltage of PV modules returns to their positive value after 0.01 s until 0.01002 s reaches a new value of 204.2 V and a new steady state value of 204.7 V, as shown in Figure 5(a). The output current of PV modules experiences the same condition, with its value fluctuating after 0.01 s and stabilising at a new steady state of 5.722 A ((6.652+4.792):2= 5.722A), as shown in Figure 5(b). The changes in the output voltage, current, and power of PV modules are controlled by the P&O algorithm to determine the possibility of pulse waves in the PWM generator.

Figure 6(a) shows the pulse wave as the output signal of the PWM generator, as shown in Figure 3, and Figure 6(b) shows the pulse wave, which is inverted by NOT gate (using a block set of logical operators) from the output signal of PWM generator. Both pulse waves are applied to the gate terminal of MOSFETs in the circuit of the half H-bridge inverter. The first pulse wave has a positive level, and the second one has a negative level every 0.0001 s. The output voltage and current of PV modules affect the pulse waves. The output voltage of PV modules drops because of reduced solar irradiance at 0.01 s and fluctuates until 0.01002 s (refer to Figure 5(a)). This condition affects the pulse waves as the output signal of the PWM generator. The patterns of pulse waves exhibit a noticeable change after 0.01 s compared to before that time, as shown in Figure 6. However, they still maintain a frequency of 5000 Hz or a period of 0.000 2 s for the duty cycle of 50%. This range indicates that the P&O algorithm can control the change value of the output voltage of PV modules well.

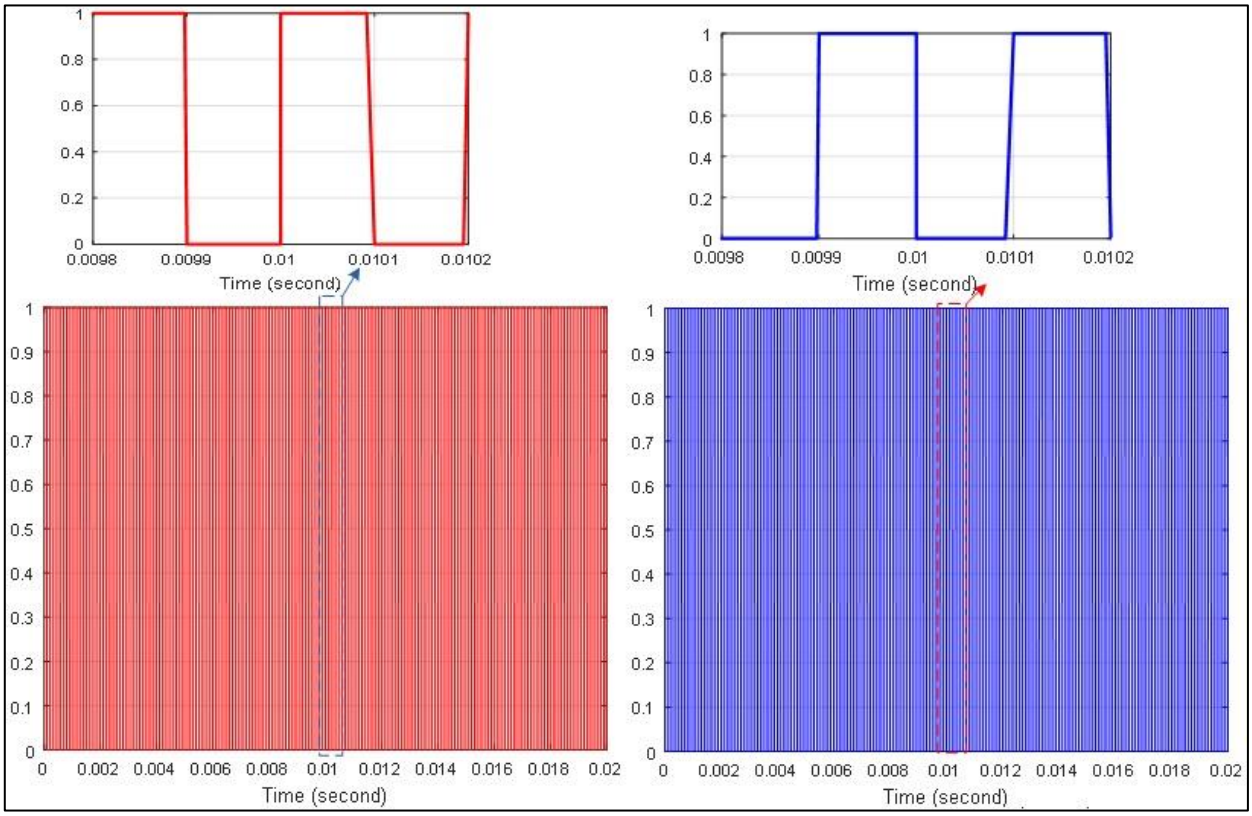


(a) (b)

**Fig. 6.** Pulse waves as output signal of PWM generator (a) Pulse wave S1 (b) Pulse wave S2

### *3.2 The WSPT Performance*

The voltage level created by the transmitting coil varies is directly proportional to the output voltage of PV modules. It means that the increased output voltage of PV modules leads to a higher voltage level produced by the transmitting coil. Meanwhile, the voltage level generated by the

transmitting coil is also reduced due to a lower output voltage from PV modules. The total output voltage of PV modules is directly proportional to the solar irradiance reaching its surface. Thus, the higher solar irradiance causes the higher output voltage of PV modules and the voltage level generated by the transmitting coil. Likewise, decreased solar irradiance leads to a reduction in the output voltage of PV modules and also in the voltage level generated by the transmitting coil.

The solar irradiance of 1000 W/m$^2$ and temperature of 25 $^o$C, as shown in Figure 4, has generated the PV module total output voltage of 233.6 V, as shown in Figure 5. The half H-bridge inverter converts this voltage to an AC voltage waveform on the transmitting coil with its maximum voltage of 150.2 V or its rms voltage of 106.2 V and its frequency of 5000 Hz, as shown in Figure 7(a). The transmitting coil generates a magnetic field for 0.01 s due to the AC current flowing through it. Upon reaching the receiving coil, the magnetic field causes an induced voltage waveform to appear, peaking at 73.48 V or having an rms voltage of 51.96 V and operating at a frequency of 5000 Hz, as shown in Figure 7(b).

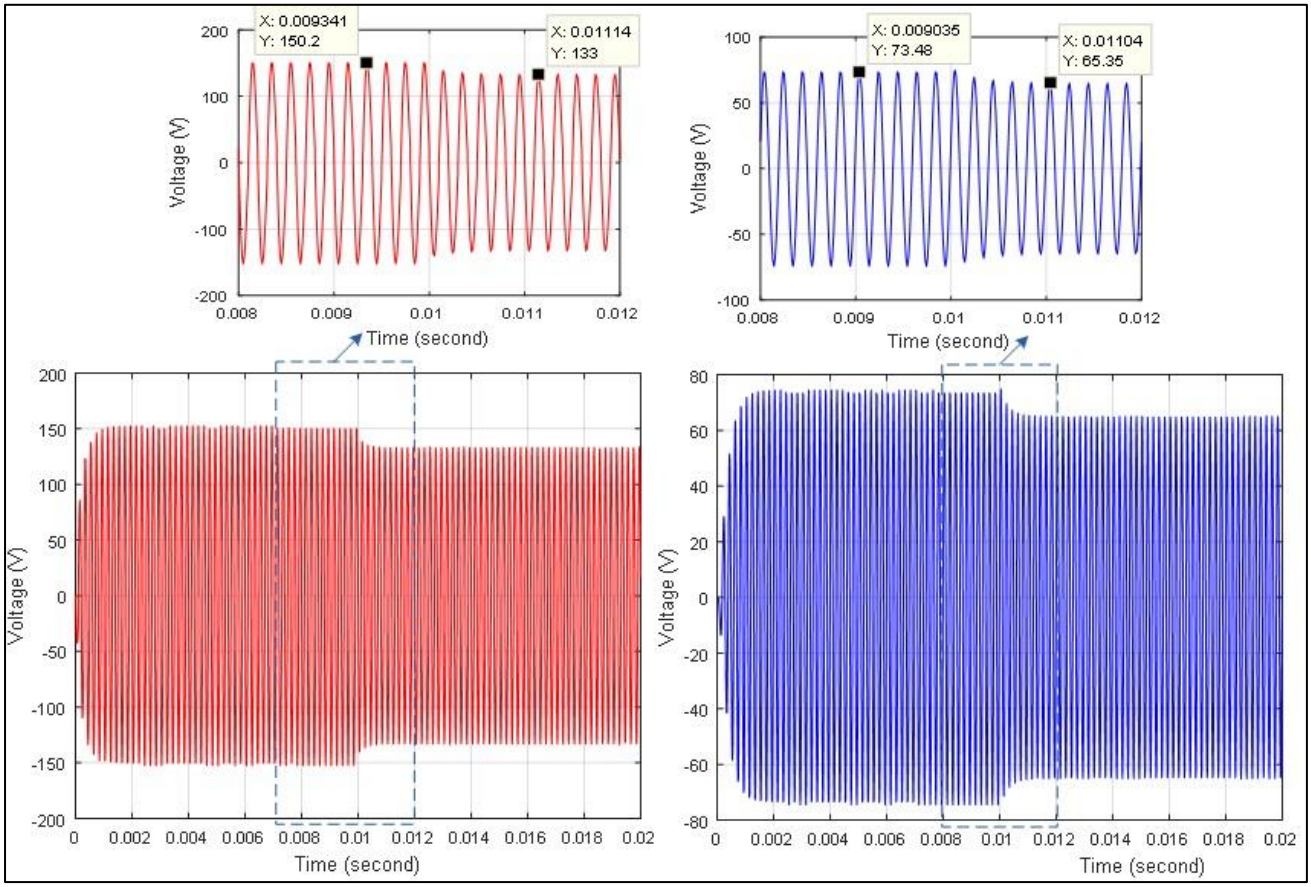


(a) Transmitting circuit (b) Receiving circuit

**Fig. 7.** Voltage waveform generated by two circuit (a) Transmitting (b) Receiving

While the total output voltage of the PV module occurs at a transient value at the time of 0.01 s, as shown in Figure 5(a), the voltage waveform on the transmitting and receiving coil does not occur at a transient voltage at the time of 0.01 s as shown in Figure 7. This observation indicates that the P&O algorithm can control the total output voltage of the PV module supplied to the half H-bridge inverter and transmitting coil well. The decreasing solar irradiance of 100 W/m$^2$ after the time of 0.01 s gives the voltage waveform generated by the transmitting coil a maximum voltage of 133 V or rms

voltage of 94.04 V, as shown in Figure 7(a). It gives the voltage waveform induced on the receiving coil with a maximum voltage of 65.35 V or rms voltage of 46.21 V, as shown in Figure 7(b).

The WSPT has transmitted the total output power of PV modules from the transmitting coil to the receiving coil. The AC power arriving at the receiving coil can be found based on the AC voltage and current waveform induced and flowed on and through the receiving coil, as shown in Figure 8. First, the difference in phase between the voltage and current waveform should be calculated. If the difference is observed at 0.008191 s, the AC voltage waveform could be observed with the AC current waveform at 0.008341 s. It means that the time difference is 0.00015 s (0.008341 s - 0.008191 s). Since the period of waveforms is 0.0002 s for reaching the angle of 360$^o$, the phase difference between the voltage and current waveform is 270$^o$. The AC voltage waveform leads the AC current waveform by 270$^o$; conversely, the AC current waveform lags behind the AC voltage waveform by 90$^o$ degrees, as depicted in Figure 8.

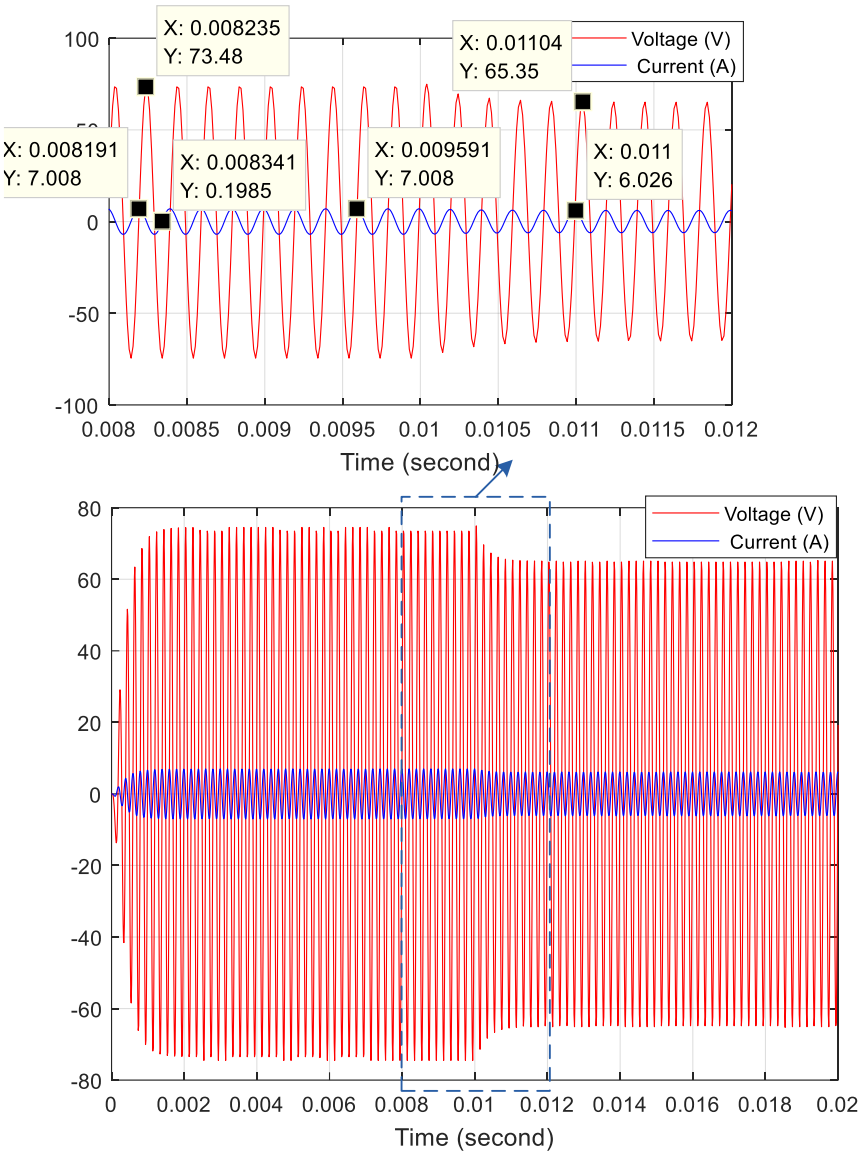


**Fig. 8.** Voltage and current waveforms on the receiving circuit

For the condition of solar irradiance of 1000 W/m$^2$ and temperature of 25 $^o$C at the time of 0 s to 0.01 s, where the rms voltage and current are 106.2 V and 4.96 A (refer Figure 8), respectively, the active power is 0 W (106.2 V x 4.96 A x cos 90$^o$ ) and the reactive power is 526.75 VAR (106.2 V x 4.96 A x sin 90$^o$ ). Moreover, for the condition of solar irradiance of 100 W/m$^2$ and temperature of 25 $^o$C at the time of 0.01 s to 0.02 s, where the rms voltage and current are 46.21 V and 4.26 A (refer Figure 8), respectively, the active power is 0 W (46.21 V x 4.26 A x cos 90$^o$ ) and the reactive power is 196.85 VAR (46.21 V x 4.26 A x sin 90$^o$ ).

## 4. Conclusions

A control strategy based on the P&O algorithm has been proposed to control the PV modules' total output voltage and current. The PWM generator's signal input generates pulse waves to drive the MOSFETs in the half H-bridge inverter of the wireless solar power transfer (WSPT) system. The system was simulated using MATLAB SIMULINK, and the change of solar irradiance, PV modules, and WSPT performances was observed and analysed. Some conclusion statements can be highlighted below.

Solar irradiance affects the performance of PV modules and WSPT. Higher solar irradiance leads to higher output voltage of PV modules and the voltage level generated by the transmitting coil. Likewise, lower solar irradiance causes the lower output voltage of PV modules and voltage level generated by the transmitting coil.

The P&O algorithm can control the pulse waves and the input function of the total output voltage and power change. During a negative transient caused by a decrease in solar irradiance from 1000 W/m$^2$ to 100 W/m$^2$, the total output voltage and power drop below zero. This results in the total output voltage reaching -2000 V due to potential induced degradation (PID) in the PV modules, while the total output power also falls below zero. When the change in P and the change in V are less than 0, it decreases the duty cycle value, $D$ (calculated as the old duty cycle, $D_{old}$, minus the change in duty cycle, $\Delta D$). This condition allows for the appropriate generation of a pulse wave on the PWM generator to control the gate terminal of MOSFETs in the half H-bridge inverter. The voltage waveform on the transmitting and receiving coil is not transient when the total output voltage and power have negative transient values. It shows that the P&O algorithm effectively regulates the overall output voltage of the PV module sent to the half H-bridge inverter and transmitting coil.

## Acknowledgement

This research was funded by a grant number of 071/E5/PG.02.00.PL/2023 from the Indonesian Ministry of Education, Culture, Research and Technology under a University Superior Basic Research grant. A good research collaboration has been conducted between Universiti Malaysia Perlis (UniMAP) and Universitas Prima Indonesia (UNPRI) to complete the research.

## References

[1] Feng, Yu, Xueli Zhang, Yue Jia, Ningbo Cui, Weiping Hao, Hongyu Li, and Daozhi Gong. "High-resolution assessment of solar radiation and energy potential in China." *Energy Conversion and Management* 240 (2021): 114265. https://doi.org/10.1016/j.enconman.2021.114265

[2] Vahdatikhaki, Faridaddin, Meggie Vincentia Barus, Qinshuo Shen, Hans Voordijk, and Amin Hammad. "Surrogate modelling of solar radiation potential for the design of PV module layout on entire façade of tall buildings." Energy and Buildings 286 (2023): 112958. https://doi.org/10.1016/j.enbuild.2023.112958

[3] Tanu, Michael, William Amponsah, Bashiru Yahaya, Enoch Bessah, Samuel Owusu Ansah, Cosmos Senyo Wemegah, and Wilson Agyei Agyare. "Evaluation of global solar radiation, cloudiness index and sky view factor as potential indicators of Ghana's solar energy resource." *Scientific African* 14 (2021): e01061. https://doi.org/10.1016/j.sciaf.2021.e01061

[4] Irwanto, M., H. Alam, M. Masri, B. Ismail, W. Z. Leow, and Y. M. Irwan. "Solar energy density estimation using ANFIS based on daily maximum and minimum temperature." *International Journal of Power Electronics and Drive Systems* 10, no. 4 (2019): 2206. http://doi.org/10.11591/ijpeds.v10.i4.pp2206-2213.

[5] Nwokolo, Samuel Chukwujindu, Solomom Okechukwu Amadi, Anthony Umunnakwe Obiwulu, Julie C. Ogbulezie, and Effiong Ekpenyong Eyibio. "Prediction of global solar radiation potential for sustainable and cleaner energy generation using improved Angstrom-Prescott and Gumbel probabilistic models." *Cleaner Engineering and Technology* 6 (2022): 100416. https://doi.org/10.1016/j.clet.2022.100416

[6] Mi, Peiyuan, Jili Zhang, Jin Gao, and Youhua Han. "Study on optimal allocation of solar photovoltaic thermal heat pump integrated energy system for domestic hot water." *Renewable Energy* 219 (2023): 119433. https://doi.org/10.1016/j.renene.2023.119433

[7] dos Santos, Wanderley Sena, Pedro Ferreira Torres, Alaan Ubaiara Brito, Marcos André Barros Galhardo, and Wilson Negrão Macêdo. "A novel fuzzy controller for photovoltaic pumping systems driven by general-purpose frequency converters." *Sustainable Energy Technologies and Assessments* 40 (2020): 100758. https://doi.org/10.1016/j.seta.2020.100758

[8] Irwanto, Muhammad, W. Z. Leow, Baharuddin Ismail, N. H. Baharudin, R. Juliangga, Hermansyah Alam, and M. Masri. "Photovoltaic powered DC-DC boost converter based on PID controller for battery charging system." In *Journal of Physics: Conference Series*, vol. 1432, no. 1, p. 012055. IOP Publishing, 2020. https://doi.org/10.1088/1742-6596/1432/1/012055.

[9] Irwanto, M., N. Gomesh, B. Ismail, H. Alam, M. Masri, and B. S. Kusuma. "Performance of nine-level transformerless photovoltaic powered inverter (TPVPI) using technique of equal maximum phase delay time." In *Journal of Physics: Conference Series*, vol. 1529, no. 4, p. 042096. IOP Publishing, 2020. https://doi.org/1%200.1088/1742-6596/1529/4/042096.

[10] Irwanto, M., N. Gomesh, Y. M. Irwan, B. Ismail, W. Z. Leow, S. Hardi, K. Saleh, H. Alam, and Suwarno. "The Technique of Voltage Level Time Division Based on Maximum Pulse Width to Reduce Total Harmonic Distortion on Multilevel Transformerless Photovoltaic Inverter (MLTPVI) System." *Journal of Electrical Engineering & Technology* 17, no. 3 (2022): 1715-1730. https://doi.org/10.1007/s42835-021-00995-z.

[11] Irwanto, M., Y. T. Nugraha, N. Hussin, I. Nisza, D. Perangin-Angin, and H. Alam. "Modelling of Wireless Power Transfer System Using MATLAB SIMULINK." In *2022 IEEE 13th Control and System Graduate Research Colloquium (ICSGRC)*, pp. 21-24. IEEE, 2022. https://doi.org/10.1109/ICSGRC55096.2022.9845181

[12] Irwanto, M., Y. T. Nugraha, N. Hussin, and I. Nisja. "Effect of Temperature and Solar Irradiance on the Performance of 50 Hz Photovoltaic Wireless Power Transfer System." *Jurnal Teknologi* 85, no. 2 (2023): 53-67. https://doi.org/10.11113/jurnalteknologi.v85.18872

[13] Rozak, Ojak Abdul, Mohd Zamri Ibrahim, Muhamad Zalani Daud, Syaiful Bakhri, and Tri Eka Oktavian. "Case Study of the Effect of Tilt Angle on Output Power and Efficiency of Photovoltaic Using Two Solar Irradiation Measurement Methods." *Journal of Advanced Research in Applied Sciences and Engineering Technology* 38, no. 1 (2024): 25-36. https://doi.org/10.37934/araset.38.1.2536.

[14] Triyanto, Aripin, NoraAini Ali, Hasiah Salleh, Ojak Abdul Rozak, Mustakim Dikri, and Norhafiza Ilyana Yatim. "Analysis Of Voltage and Current Performance of 100 WP Solar Panel Using Matlab Simulink R2021a." *Journal of Advanced Research in Applied Sciences and Engineering Technology* 34, no. 2 (2023): 18-29. https://doi.org/10.37934/araset.34.2.1829

[15] Irwanto, M., M. Badruzzaman Ali, Y. T. Nugraha, B. Ismail, I. Nisja, and W. Z. Leow. "Analysis on the Effect of DC Current Changes on the Magnetic Field of Wireless Power Transfer." In *2023 IEEE 14th Control and System Graduate Research Colloquium (ICSGRC)*, pp. 186-191. IEEE, 2023. https://doi.org/10.1109/ICSGRC57744.2023.10215406

[16] de Miranda, Caio M., and Sérgio F. Pichorim. "A Three-Coil Wireless Power Transfer System using Self-Resonant Open-Bifilar Coils." *AEU-International Journal of Electronics and Communications* 154 (2022): 154300. https://doi.org/10.1016/j.aeue.2022.154300

[17] Makhetha, Molefi J., Elisha D. Markus, and Adnan M. Abu-Mahfouz. "Efficient wireless power transfer via self-resonant Conformal Strongly Coupled Magnetic Resonance for wireless sensor networks." *Energy Reports* 8 (2022): 1358-1367. https://doi.org/10.1016/j.egyr.2022.08.261

[18] Wen, Feng, Xiang Zhang, Qiang Li, Dashang Zhang, Guofeng Li, Shuqi Wu, Zhijun Yao, and Kaiming Yu. "Research on coil positioning method and magnetic field orientation strategy of wireless power transfer system." *Energy Reports* 9 (2023): 353-361. https://doi.org/10.1016/j.egyr.2023.09.021

[19] Hyun, Seungmin, Hongguk Bae, and Sangwook Park. "Characteristics analysis of resonance-based wireless power transfer using magnetic coupling and electric coupling." *Engineering Science and Technology, an International Journal* 42 (2023): 101419. https://doi.org/10.1016/j.jestch.2023.101419

[20] Leng, Yang, Derong Luo, Zhongqi Li, and Fei Yu. "Coupling coefficient calculation and optimization of positive rectangular series coils in wireless power transfer systems." *Heliyon* 9, no. 10 (2023). https://doi.org/10.1016/j.heliyon.2023.e21121.

[21] Butar-Butar, A. H., J. H. Leong, and M. Irwanto. "Effect of DC voltage source on the voltage and current of transmitter and receiver coil of 2.5 kHz wireless power transfer." *Bulletin of Electrical Engineering and Informatics* 9, no. 2 (2020): 484-491. https://doi.org/10.11591/eei.v9i2.2060.

[22] Faiz, Muhammad Izzul Syafiq, Md Rabiul Awal, Md Rubel Basar, Nurul Adilah Abdul Latiff, Muhammad Syarifuddin Yahya, and Shakir Saat. "A Comparative Review on Acoustic and Inductive Power Transfer." *Journal of Advanced Research in Applied Sciences and Engineering Technology* 44, no. 1 (2025): 188-224. https://doi.org/10.37934/araset.44.1.188224.

[23] Saifizi, M., M. I. Fahmi, M. Othman, Wan Azani Mustafa, M. Z. Aihsan, M. R. Manan, and Azri A. Aziz. "Implementation of Two-Stage Multilevel Inverter System Using PIC Controller." *Journal of Advanced Research in Applied Sciences and Engineering Technology* 28, no. 2 (2022): 41-55. https://doi.org/10.37934/araset.28.2.4155.

[24] Kamarudin, Nornaim, Ahmad Asri Abd Samat, Mohammad Faridun Naim Tajudin, Muhammad Khusairi Osman, Saodah Omar, and Irni Hamiza Hamzah. "Design of Buck Converter Based on Maximum Power Point Tracking for Photovoltaic Applications." *Journal of Advanced Research in Applied Sciences and Engineering Technology* 39, no. 2 (2024): 242-257. https://doi.org/10.37934/araset.39.2.242257.

[25] Pilakkat, Deepthi, and S. Kanthalakshmi. "An improved P&O algorithm integrated with artificial bee colony for photovoltaic systems under partial shading conditions." *Solar Energy* 178 (2019): 37-47. https://doi.org/10.1016/j.solener.2018.12.008